HHS Public Access

Author manuscript

Plant Cell Environ. Author manuscript; available in PMC 2020 December 18.

Published in final edited form as:

Plant Cell Environ. 2019 September ; 42(9): 2664–2680. doi:10.1111/pce.13569.

The tomato Arp2/3 complex is required for resistance to the powdery mildew fungus *Oidium neolycopersici*

Guangzheng Sun[#1], **Chanjing Feng**[#1], **Jia Guo**[1], **Ancheng Zhang**[1], **Yuanliu Xu**[1], **Yang Wang**[1], **Brad Day**[2,3], **Qing Ma**[1]

[1]State Key Laboratory of Crop Stress Biology for Arid Areas, College of Plant Protection, Northwest A&F University, Yangling, China

[2]Department of Plant, Soil and Microbial Sciences, Michigan State University, East Lansing, Michigan

[3]Plant Resilience Institute, Michigan State University, East Lansing, Michigan

[#] These authors contributed equally to this work.

Abstract

The actin-related protein 2/3 complex (Arp2/3 complex), a key regulator of actin cytoskeletal dynamics, has been linked to multiple cellular processes, including those associated with response to stress. Herein, the *Solanum habrochaites ARPC3* gene, encoding a subunit protein of the Arp2/3 complex, was identified and characterized. *ShARPC3* encodes a 174-amino acid protein possessing a conserved P21-Arc domain. Silencing of *ShARPC3* resulted in enhanced susceptibility to the powdery mildew pathogen *Oidium neolycopersici* (*On*-Lz), demonstrating a role for *ShARPC3* in defence signalling. Interestingly, a loss of *ShARPC3* coincided with enhanced susceptibility to *On*-Lz, a process that we hypothesize is the result of a block in the activity of SA-mediated defence signalling. Conversely, overexpression of *ShARPC3* in *Arabidopsis thaliana*, followed by inoculation with *On*-Lz, showed enhanced resistance, including the rapid induction of hypersensitive cell death and the generation of reactive oxygen. Heterologous expression of *ShARPC3* in the *arc18* mutant of *Saccharomyces cerevisiae* (i.e., Δ*arc18*) resulted in complementation of stress-induced phenotypes, including high-temperature tolerance. Taken together, these data support a role for ShARPC3 in tomato through positive regulation of plant immunity in response to *O. neolycopersici* pathogenesis.

Keywords

actin cytoskeleton; Arp2/3 complex; ARPC3; powdery mildew; resistance; *Solanum habrochaites*

Correspondence: Brad Day, Department of Plant, Soil and Microbial Sciences, Michigan State University, East Lansing, MI 48824. bday@msu.edu, Qing Ma, State Key Laboratory of Crop Stress Biology for Arid Areas, College of Plant Protection, Northwest A&F University, Yangling 712100, China. maqing@nwsuaf.edu.cn.

SUPPORTING INFORMATION

Additional supporting information may be found online in the Supporting Information section at the end of the article.

1 | INTRODUCTION

Tomato powdery mildew, *Oidium neolycopersici*, is an obligate biotrophic fungus that can parasitize more than 60 plant species in 13 families, including members of the *Solanaceae* (Jones, Whipps, & Guu, 2001). Upon infection of a susceptible host, *O. neolycopersici* causes powdery white lesions on the adaxial tomato leaf surface, abaxial surfaces, petioles, and the calyx; only the fruit remains uninfected. Pathogen infection typically affects leaves of the host plant, causing up to 50% yield losses (fruit) as a result of loss of vigour (Roberts, Momol, & Pernezny, 2002), and has caused devastating epidemics from Europe to North and South America, as well as in Asia (Lebeda et al., 2014). At present, chemical control remains the primary method to manage tomato powdery mildew in greenhouse production; however, chemical fungicide application introduces numerous inherent risks, including the development of pathogen resistance and the accumulation of toxic residues in fruit, both of which pose potential risks to the environment (Nakajima & Akutsu, 2014).

Plants defence signalling in response to bacterial and fungal pathogen infection is mediated by at least two primary nodes of the host innate immune system (Jones & Dangl, 2006). The first, pathogen-associated molecular pattern (PAMP)-triggered immunity (PTI), is often sufficient to protect plants against most pathogens and is often described as a mechanism of nonhost (basal) resistance (Marcel et al., 2008). In response to PTI, pathogens evolved mechanisms counter host defences, a process that functions via the delivery of virulence molecules which target a variety of host functions, including immune signalling. To counter this pathogen virulence function, plants evolved to recognize and respond to effector delivery, a process known as effector-triggered immunity (ETI). In short, ETI results in the activation of robust immune signalling, often characterized by localized cell death (i.e., the hypersensitive response [HR]) and the subsequent halt of pathogen growth and proliferation (Chisholm, Coaker, Day, & Staskawicz, 2006).

To date, most of the cloned resistance (*R*) genes encode proteins with an N-terminal nucleotide-binding site (NBS) and C-terminal leucine-rich repeats (LRRs; Takken, Albrecht, & Tameling, 2006). In wild tomato species, several *R* genes have been identified, including six monogenic genes comprising five dominant (*Ol-1*, *Ol-3*, *Ol-4*, *Ol-5*, and *Ol-6*), one recessive (*ol-2*) loci, and three polygenic resistance quantitative trait loci (QTLs; Bai et al., 2005; Bai, Huang, Van Der Hulst, Meijer-Dekens, & Bonnema, 2003). In brief, *Ol-4*-mediated resistance relies on the salicylic acid (SA) pathway, whereas *Ol-1* and *Ol-qtls* require ethylene (ET) to promote delayed cell death during powdery mildew resistance, and jasmonic acid (JA) deficiency can compromise resistance mediated by *ol-2* (Bai et al., 2005; Bai et al., 2003; Ciccarese, Amenduni, Ambrico, & Cirulli, 2000; Lindhout, Pet, & van der Beek, 1994; Lindhout, van der Beek, & Pet, 1994; Pei et al., 2011). In all instances, resistance to *O. neolycopersici* is associated with the induction of the HR, with a high frequency of necrosis in epidermal cells accompanying H_2O_2 accumulation induced by the fungal haustoria (Bai et al., 2005). Interestingly, when cells undergo the HR, uninfected neighbouring cells show an accumulation of focal actin microfilaments (AFs; Kobayashi, Kobayashi, & Hardham, 1994).

The eukaryotic cytoskeleton forms a contiguous network within all cells and includes microtubules (MT) and AF systems, both of which are associated with the function of numerous cellular processes (Day, Henty, Porter, & Staiger, 2011; Kim, Park, Kim, & Hwang, 2005; Li & Day, 2019; Sparkes, Runions, Hawes, & Griffing, 2009; Yokota et al., 2009). In short, MTs are hypothesized to play a role in maintaining cell polarity, whereas AFs ensure the targeted delivery of vesicles that carry plasma membrane and cell wall components to the site of growth (Mathur & Hülskamp, 2002). Additionally, AFs support the formation of penetration barriers by recruiting defence-related products to the subcellular site of fungal attack (Opalski, Schultheiss, Kogel, & Hückelhoven, 2005). As a putative mechanism underpinning actin-associated defence signalling, work by Henty-Ridilla et al. (2013) and Shimono, Higaki, et al. (2016) noted that early transient accumulation of actin (i.e., increased density and decreased filament bundling) is associated with the activation of PTI. Additional evidence points to the requirement for a suite actin-binding proteins (ABPs), including the actin-related protein 2 and 3 (Arp2/3) complex, profilin, and actin depolymerizing factors (ADF; reviewed in Porter & Day, 2015).

A key step in AF organization is actin nucleation, the key rate-limiting step necessary to ensure proper filaments formation (Campellone & Welch, 2010); this process is regulated by the Arp2/3 complex (Chesarone & Goode, 2009). The Arp2/3 complex contains seven subunits, including two actin-related proteins (ARP2 and ARP3) and five unrelated subunits (Machesky et al., 1999; Machesky, Atkinson, Ampe, Vandekerckhove, & Pollard, 1994). In eukaryotes, this complex facilitates branched actin network nucleation associated with regions of the plasma membrane (Pollard & Borisy, 2003; Weaver, Young, Lee, & Cooper, 2003) and is involved in actin polymerization-mediated motility of organelles (Machesky et al., 1999; Welch, Holtzman, & Drubin, 2002). Interestingly, Mathur, Mathur, Kernebeck, and Hülskamp (2003) found that expansion growth in Arabidopsis requires ARP2/3 activity, and its loss results in inefficient fine F-actin formation, leading to enhanced F-actin aggregation and bundling.

At a fundamental level, the Arp2/3 complex polymerizes new AFs in response to suite of signals, including those associated with growth, development, and response to external stimuli (Pantaloni, le Clainche, & Carlier, 2001; Pollard, Blanchoin, & Mullins, 2000; Takenawa & Miki, 2001). Interestingly, the seven subunits serve distinct roles in numerous developmental processes. For example, Arp2 is essential for membrane association (Kotchoni et al., 2009), whereas Arp3 is primarily associated with sites of actin nucleation (Maisch, Fiserova, Fischer, & Nick, 2009). Further research also demonstrated that deletion of *ARPC1* or *ARPC2* resulted in lethality and severe reductions in viability in *Saccharomyces cerevisiae*. In plants, Mathur, Mathur, Kernebeck et al. (2003); Mathur, Mathur, Kirik, et al. (2003) observed that loss-of-function mutants in Arabidopsis ARP3 or ARPC5 leads to shorter and sometimes sinuous root hairs. As a function of plant immunity, recent work by Qi et al. (2017) demonstrated that *Ta*ARPC3 is a key subunit of the Arp2/3 complex that is required for wheat resistance against *Puccinia striiformis* f. sp. *tritici*.

In the current study, we found that expression of *ShARPC3* was significantly up-regulated during an incompatible host-pathogen interaction, suggestive of a role for *ShARPC3* in plant defence signalling and immunity. This is significant, as a defined role for Arp2/3 signalling

during plant pathogenesis by fungal pathogens has not been described. Using the model plant tomato and infection by the powdery mildew pathogen *O. neolycopersici*, we describe a function for *ShARPC3* during infection and defence signalling in tomato. In total, the current study contributes to a broader understanding of the role of the Arp2/3 complex in pathogen defence signalling, and moreover, sheds light on the regulation of this complex in growth, development, and response to stress.

2 | RESULTS

2.1 | Identification and sequence analysis of tomato ARPC3

A tomato 525-bp homologue of actin-related protein was isolated from tomato LA1777 by homology-based cloning, and the obtained cDNA was designated as *ShARPC3*. Blast analysis of *ShARPC3* nucleotide sequence in the Tomato Genome CDS (ITAG release 3.20) database revealed that one copy was present, localized on chromosome 7. The predicted ORF of *ShARPC3* encodes a protein of 174 amino acid with a predicted molecular weight of 21 kDa. As shown in Figure 1a, phylogenetic analysis of *Sh*ARPC3 with other tomato ARP2/3 complex members and other species ARP2/3 complex members revealed that *Sh*ARPC3 clusters with *At*ARPC3 (AT1G60430) and *Nt*ARPC3 (XM_009610279), all of which are members of actin-related proteins in dicotyledons. Amino acid sequences alignment of *Sh*ARPC3 with *At*ARPC3, *Ns*ARPC3 (XP_009791878), *Nt*ARPC3 (XP_009608574), *Bn*ARPC3 (XP_022548276), *Sb*ARPC3 (XP_002451839), *Vr*ARPC3 (XP_014510301), and *Os*ARPC3 (XP_015626361) predicts that *ShARPC3* encodes a protein with unique conserved domains also found in the ARP2/3 complex-containing subunit ARPC3 (Figure 1b). In silico-based sequence analysis revealed that *Sh*ARPC3 has high sequence similarity to *At*ARPC3 and *Nt*ARPC3, with identities of 86% and 93%, respectively. SMART and RCSB PDB analyses revealed that *Sh*ARPC3 possesses a conserved Pfam:P21-Arc domain (amino acids 1–173), one glycyl lysine isopeptide (Lys-Gly; interchain with G-Cter in SUMO2)-cross-link site (amino acid 14), one phosphotyrosine-modified residue (amino acid 47), and two N6-acetyllysine-modified residues (amino acids 56 and 61). These data reveal that *Sh*ARPC3 is closely related to *At*ARPC3 and *Nt*ARPC3.

Using an in silico-based approach (e.g., STRING database analysis), we generated a predicted protein network map (Figure 1c; high confidence score = 0.982), which revealed interactions between tomato ARPC3 and numerous additional tomato proteins. As shown, tomato ARPC3 is predicted to interact with actin-related protein 2/3 complex subunit 1A (ARPC1A), ARP2/3 complex subunit 1B (ARPC1B), ARP2/3 complex subunit 2 (ARPC2), ARP2/3 complex subunit 4 (ARPC4), ARP2/3 complex subunit 5 (ARPC5), ARP2/3 complex subunit 5-like protein (ARPC5L), ARP2 (ACTR2), ARP3 (ACTR3), ARP3B (ACTR3B), and Neural Wiskott-Aldrich syndrome protein (WASL). In total, the interaction map contains a total 11 nodes with 54 edges, and further analysis indicates that all of these tomato proteins are involved in actin cytoskeletal organization, mitosis, and cytokinesis. Based on this, we hypothesize that *Sh*ARPC3 functions through dynamic interactions with other ARP2/3 complex subunits to regulate cellular morphology, as well as abiotic and biotic signalling responses.

2.2 | ShARPC3 is localized in the cytoplasm and plasma membrane in tomato protoplast

Based on the analysis above, we hypothesized that *Sh*ARPC3 is localized within multiple subcellular environments, including plasma membrane, extracellular spaces, cytoplasm, mitochondria, endoplasmic reticulum, peroxisomes, Golgi, and chloroplast (Table S4). To further determine the precise subcellular localization of *Sh*ARPC3, the *ShARPC3* ORF was fused to GFP and placed under the control of the constitutive *Cauliflower mosaic virus* 35S promoter and transiently expressed in tomato protoplasts. As shown in Figure 2, pCaMV35S:*GFP* (negative control) revealed a diffuse, non-specific cellular address, whereas cells expressing GFP-tagged ShARPC3 was localized predominantly in the cytoplasm and nucleus.

2.3 | ShARPC3 does not induce the hypersensitive cell death response nor suppress BAX-induced necrosis

To further define *ShARPC3* function, we next employed a PVX-based high-throughput transient plant overexpression system under the regulation of the 35S promoter, using *Nicotiana benthamiana*, to evaluate ARPC3 function and activity during cell death elicitation. As shown in Figure S1, infiltration of *N. benthamiana* leaves with Agrobacterium expressing pGR106:*GFP* (site “a,” CK), pGR106: *ShARPC3* (site “b”), or buffer alone (site “c”) did not result in the induction of cell death symptoms. These data indicate that ARPC3 does not possess cell death-inducing activity. To determine if the overexpression of ARPC3 can positively, or negatively, influence BAX-induced cell death, *N. benthamiana* leaves were infiltrated with Agrobacterium cells harbouring *ShARPC3* gene 24 hr prior to infiltration with the pGR106:*BAX*-harbouring cells produced cell death symptoms (Figure S1, site “e”). As expected, cell death was observed in *N. benthamiana* leaves infiltrated with Agrobacterium cells expressing pGR106:GFP:*BAX* (Figure S1, site “d”). As shown, the BAX-induced cell death response, in the presence of ARPC3, was no different than overexpression of BAX alone (Figure S1, site “f”).

2.4 | ShARPC3 is differentially induced by *On*-Lz infection

To determine the expression profile of *ShARPC3*, the mRNA accumulation of *ShARPC3* was monitored during the interaction between tomato and *On*-Lz using qRT-PCR. LA1777 plants showed resistance against *On*-Lz, whereas obvious powdery mildew disease lesions appeared in MM plants (Figure S2a). The disease indexes of MM plants were significantly higher, with lesion indices reaching 18.5 and 26.4 at 7 and 14 dpi, respectively (Figure S2b). As shown in Figure 3, during an incompatible interaction, *ShARPC3* transcripts were significantly up-regulated at 12–24 hpi, and mRNA accumulation peaked at 18 hpi, 16 times ($P < .05$) than that in control (uninoculated) plants. Additionally, *ShARPC3* transcript levels were much higher during an incompatible interaction than during a compatible interaction at all time points evaluated, except at 96 hpi. Based on this, we hypothesize that *ShARPC3* is associated with resistance of tomato against *On*-Lz infection.

2.5 | Silencing of ShARPC3 results in host susceptibility to *On*-Lz

To determine the role of *ShARPC3* during tomato infection by *On*-Lz, we used a tobacco rattle virus-induced gene silencing (TRV-VIGS)-based approach to silence *ShARPC3*

expression in LA1777. As shown in Figure 4, TRV2 (CK), TRV2:*ShPDS* (phytoene desaturase), and TRV2:*ShARPC3* plasmids were inoculated onto tomato leaves for silencing. As expected, plants inoculated with TRV2:*ShPDS* showed a photobleaching phenotype at ~30 days post-inoculation (Figure 4 a), indicating the induction of TRV-VIGS-mediated silencing. At this point (i.e., 30 dpi), all plants were inoculated with *On*-Lz, and infection phenotypes were recorded. Compared with control plants, plants carrying TRV2:*ShARPC3* showed obvious powdery mildew disease spot lesions (Figure 4a), and the disease indexes of *ShARPC3*-silenced plants were significantly higher, with lesion indices reaching 10.7 and 21.1 at 7 and 14 dpi, respectively (Figure 4b). In parallel, samples were collected to assess the efficiency of gene silencing using qRT-PCR analysis. The expression of *ShARPC3* was reduced by 60–85% at 0–72 hpi compared with control-inoculated leaves (Figure S3); *ShARPC3*-silenced efficiency peaked at 24 hpi. Based on these data, we conclude that *ShARPC3* is required for resistance to *On*-Lz.

2.6 | Silencing of ShARPC3 results in reduced defence responses following *On*-Lz inoculation

To further investigate how *ShARPC3* participates in tomato resistance to *On*-Lz, we measured the accumulation of H_2O_2 and the development of the HR at 6, 18, 24, 48, and 72 hpi via a microscopic examination of the infection process (Figure 5). As shown, a histological examination of *On*-Lz growth was performed in both control and *ShARPC3*-silenced plants by analysing the HR production rate (Figure 5a,c). We found that HR production in the *ShARPC3*-silenced plants was much less compared with the control plants at 48 and 72 hpi ($P < .05$). There were no obvious differences between TRV2-treated and *ShARPC3*-silenced plants in HR production at 18 and 24 hpi. As the infection progressed, we also observed a significant decrease in the amount of H_2O_2 accumulated in *ShARPC3*-silenced plants (leaves) at 72 hpi ($P < .05$); H_2O_2 was 0.45 times that in TRV2-treated leaves (CK; Figure 5b,d). Additionally, with the increase of haustoria formation, more invasive growth in *ShARPC3*-silenced plants was observed than in control plants. Taken together, these results indicate that a reduction in *ShARPC3* expression compromises resistance signalling in response to *On*-Lz infection.

2.7 | Effects of ShARPC3 silencing on phytohormone accumulation and PR transcript levels

To confirm the relevance of *ShARPC3* expression as a function of the activity of SA signalling pathway, we measured SA level in *ShARPC3*-silenced plants at 0–24 hpi with *On*-Lz. As shown in Figure 6a, in control plants (CK), SA content reached its highest level of 1,818.0 $\mu g \cdot g^{-1}$ at 12 hpi, >2.5 times that in *ShARPC3*-silenced plants. Additionally, SA levels were significantly lower in *ShARPC3*-silenced plants than in the control plants at all time points and higher than that at 0 hpi. We further studied pathogenesis-related (PR) *PR1b1* (*PR1*), *Glucanase A* (*PR2*), *Glucanase B* (*PR2-like*), *Chitinase 3* (*PR3*), and *Chitinase 9* (*PR3-like*) gene expression after inoculation with *On*-Lz. In *ShARPC3*-silenced plants at 24 hpi, the expressions of *PR1*, *PR2*, and *PR3* genes (SA pathway-specific gene expression markers) were significantly reduced (Figure 6b). Taken together, we posit that *ShARPC3* is required for the positive regulation of host defences, mediated in part by SA signalling.

2.8 | Overexpression of ShARPC3 functionally complements the arpc3 mutation

To test whether *ShARPC3*-based resistance occurs in Arabidopsis, we evaluated a homozygous *arpc3* mutant, an *arpc3* complementation line, and WT Col-0 plants overexpressing *ShARPC3* under the regulation of the 35S promoter and challenged them with *On*-Lz. As expected, macroscopic inspection revealed that *arpc3* plants were susceptible to *On*-Lz (Figure 7b). However, *arpc3* complementation plants, like the control plants (i.e., WT Col-0), showed only slight disease symptoms following infection. Conversely, WT Col-0 plants carrying 35S:pCAMBIA3301-*ShARPC3* showed no obvious symptoms, possibly due to the additive effect of native + transgene overexpression of *ShARPC3*. Microscopic examination revealed that resistance in *arpc3* plants carrying 35S:pCAMBIA3301-*ShARPC3* and WT Col-0 plants carrying 35S:pCAMBIA3301-*ShARPC3* was incomplete and characterized by reduced conidiophore and haustorium formation (Figure 7c–e). Compared with control plants (i.e., WT Col-0), conidiophore production was significantly higher in *arpc3* mutant plants ($P < .05$). Additionally, the growth ability of the complemented *arpc3* plants containing 35S:pCAMBIA3301-*ShARPC3* was stronger than that in the *arpc3* mutant yet weaker than that in WT Col-0 plants (Figure 7a).

2.9 | Resistance mechanisms revealed in histological and biochemical studies

To assess the impact of *ARPC3* on the response of Arabidopsis to *On*-Lz, we next investigated the host response via a microscopic examination of the infection process. To do this, we measured the development of the HR (Figure 8a,c) and the accumulation of H_2O_2 (Figure 8b,d) at 6, 18, 24, 48, and 72 hpi. As shown, we observed no significant differences in either HR development or H_2O_2 accumulation among four treatments at 6–24 hpi. However, when compared with *ShARPC3*-overexpression plants (i.e., *arpc3* complementation lines or WT Col-0 overexpression), cell death elicitation was significantly reduced in control and *arpc3* plants at 48 hpi. Moreover, we observed that HR production in *arpc3* plants was much less than that in the control plants at 72 hpi ($P < .05$). Consistent with this observation, H_2O_2 production rate was significantly lower in *arpc3* plants than that of other treatments at 48 hpi ($P < .05$). Indeed, H_2O_2 accumulation was frequently observed at levels significantly higher in mesophyll cells of *arpc3* plants carrying pCAMBIA3301-*ShARPC3* and WT Col-0 plants carrying pCAMBIA3301-*ShARPC3* than in control plants and *arpc3* mutant plants at 72 hpi. In addition to altered H_2O_2 accumulation and cell death, qRT-PCR analyses revealed that accumulation of *AtARPC3* mRNA was rapidly induced and increased significantly over time in *ShARPC3*-overexpression plants compared with *AtARPC3* mRNA levels in WT Col-0 plants (Figure S4). Conversely, the expression of *AtARPC3* was significantly lower in *arpc3* plants than that in WT Col-0 plants at 0–72 hpi. Taken together, we posit that an increase in *ShARPC3* mRNA accumulation is required for robust defence signalling in response to *On*-Lz infection.

2.10 | Heterologous expression of ShARPC3 partially rescues the arc18 mutant in *S. cerevisiae*

S. cerevisiae growth is sensitive to high temperatures, with optimum growth at 30°C. To further explore the function of *ShARPC3* in response to temperature stress, *ShARPC3* was

expressed in the *S. cerevisiae arc18* mutant strain, and transformants were grown under different temperature conditions (e.g., 24°C, 30°C, 36°C, and 42°C). As shown in Figure S5, the growth *S. cerevisiae* strain Y06714 harbouring pDR195-ShARPC3 was more robust than that of the *arpc3 S. cerevisiae* mutant carrying the empty expression vector pDR195 but was weaker than that of the WT yeast strain, BY4741. Taken together, these data demonstrate that heterologous expression of *ShARPC3* in yeast partially restores the growth at elevated temperatures, suggestive of a functional conservation between *Sh*ARPC3 and yeast ARC18 and a role in abiotic stress signalling and tolerance.

3 | DISCUSSION

Previous work demonstrated that the Arp2/3 complex is required for actin polymerization and the formation of branched actin networks (Welch, Iwamatsu, & Mitchison, 1997). In the current study, and as a function of plant defence signalling, our data reveal a new role for *Sh*ARPC3 during tomato infection by the powdery mildew pathogen *On*-Lz. This is significant, as the current study provides insight into the network of processes that are activated upon pathogen perception and immune signalling. Indeed, we observed that accumulation of *ShARPC3* was rapidly induced during an incompatible interaction, suggesting that *ShARPC3* accumulation might be an early defence activation signal which associated with the stimulation of a large number of primary haustoria. Conversely, and in support of this hypothesis, in the compatible interaction, the expression of *ShARPC3* was down-regulated at all time points—with the exception of 96 hpi—as compared with 0 hpi. In total, these data support the hypothesis that *Sh*ARPC3 is a key regulator of the disease resistance response in tomato against *O. neolycopersici*.

Using a VIGS-based approach, further support for this was revealed by silencing of *ShARPC3* in LA1777, followed by infection with *On*-Lz, led to the development of susceptibility, indicating that *ShARPC3* is a key component of the Arp2/3 complex-mediated disease resistance response in tomato against *O. neolycopersici*. Although it remains to be investigated, we suggest that this process is likely associated with actin polymerization catalysed by the Arp2/3 complex, and moreover, functions as a pivotal component in the plant defence signalling cascade (Tian et al., 2009; Welch & Mullins, 2002; Zhang et al., 2017).

In the current study, we provide evidence for a role for *ShARPC3* as a resistance-associated gene activated in response to *On*-Lz infection. We observed that *arpc3* mutant complementation with a 35S-expressing *ShARPC3* construct restores *On*-Lz resistance; in WT Col-0 plants carrying pCAMBIA3301-*ShARPC3*, we observed enhanced resistance to *On*-Lz compared with *arpc3* plants carrying pCAMBIA3301-*ShARPC3* (Figure 7b). Based on this, it seems plausible that in the case of complementation of *arpc3* by *ShARPC3*, there is also a quantitative effect due to differing levels of *ShARPC3* expression in individual transformants, leading to the observation that *ShARPC3* only partially restores resistance. In this study, compared with nonsilenced resistant LA1777 plants, which show a rapid induction of the HR and H_2O_2 accumulation, *ShARPC3*-silenced plants showed a markedly slower HR and H_2O_2 accumulation, responses that coincide with a loss of *On*-Lz resistance. These observations support our previous findings that transcriptomic differences between

compatible and incompatible interactions of tomato and *O. neolycopersici* are mainly in timing (Li et al., 2006; Pei et al., 2011). Furthermore, it also indicates that the expression level of *ShARPC3* correlates with the level of *On*-Lz induced HR and H_2O_2 accumulation in tomato, implying that the Arp2/3 complex plays a role in the tomato-*O. neolycopersici* interaction through adjusting the level, and amplitude, of the HR and H_2O_2 accumulation.

As a possible, yet undefined, mechanism underpinning this response, numerous reports have observed that changes in cytoskeletal organization lead to reactive oxygen bursts and subsequent cell death (Gourlay & Ayscough, 2005; Fu et al., 2014; Shimono, Lu, et al., 2016; Zhang et al., 2017). Indeed, rearrangement of the plant actin cytoskeleton has been correlated with the activation of defence signalling; most notably, the generation of ROS, changes in gene expression and formation of papillae at the site of penetration (Gourlay & Ayscough, 2005; Huot et al., 1998; Wang et al., 2009). Taken together with our observation of the impact of *ShARPC3* overexpression in Arabidopsis, we posit a role for *Sh*ARPC3 as a positive regulator of immunity in response to *On*-Lz infection.

Our data describe a role for *Sh*ARPC3 associated with SA signalling (Lan et al., 2013; Li & Zou, 2017). Indeed, we observed that SA level was elevated in WT plants following inoculation and was reduced in *ShARPC3*-silenced plants. And tomato can receive the stimuli from *On*-Lz quickly and trigger SA-inducible PR proteins (PR1, PR2, and PR3) to protect themselves from being invaded, because the strength of *PR* gene expression has been linked to penetration resistance (Molitor et al., 2011; Peterhänsel, Freialdenhoven, Kurth, Kolsch, & Schulze-Lefert, 1997; Van Verk, Pappaioannou, Neeleman, Bol, & Linthorst, 2008). Based on these observations, it is reasonable to assume that SA is involved in the development of resistance to *On*-Lz in tomato, and that modulation of this defence hormone induces the expression of several defence-related genes (e.g., β−1,3-glucanase and chitinase) as observed in other host-pathogen systems (e.g., Mouekouba et al., 2014; Sun et al., 2017). In agreement with our findings, Sun et al. (2017) reported that *Glucanase-A*, *Glucanase-B*, *Chitinase-3*, *Chitinase-9*, and *PR-1* transcripts significantly changed in the ε-poly-L-lysine-treated + *Botrytis cinerea* infected tomato plants. Interestingly, no significant fitness costs in terms of reduced growth were observed *via ShARPC3* silencing, thus making this gene a promising target for mutagenesis to obtain suitable *ShARPC3* alleles for disease resistance breeding in tomato. However, the growth ability of Arabidopsis *arpc3* mutant was weaker than that in WT Col-0 plants. We speculate that the decrease of disease resistance in *arpc3* mutant is due to blocked SA signalling pathways rather than changes in plant size. Rops, as upstream regulators of ARP2/3 complex, can affect the polymerization of microfilament skeleton (Jaffe & Hall, 2005). Poraty-Gavra et al. (2013) indicated that the morphological aberration of Arabidopsis *rop6* mutant results from perturbations that are independent from the SA-associated response. These perturbations uncouple SA-dependent defence signalling from disease resistance execution. Based on the sum of the data presented herein, we hypothesize that *Sh*ARPC3 may function in a similar manner, and moreover, the current study points to a role for the Arp2/3 signalling platform in the control of multiple intercellular signalling processes that are required for immune activation and general stress response signalling.

4 | MATERIALS AND METHODS

4.1 | Strains and plant growth

O. neolycopersici Lanzhou strain (*On*-Lz) was isolated from tomato plants in Gansu Province, China, and was kindly provided by the College of Plant Protection, Northwest A&F University, Yangling, China. The isolate was preserved and propagated on tomato (cv. Money-maker [MM]) in an environmentally controlled growth chamber at 20 ± 3°C with 70 ± 5% humidity and a 16 hr photoperiod.

The *S. cerevisiae* diploid mutant strain Y06714 (MATa; *ura310*; *leu210*; *his311*; *met1510*; YLR370c::kanMX4) was grown on SC-U medium at 30°C, and the WT strain BY4741 (MATa; *his311*; *leu210*; *met1510*; *ura310*) was grown on yeast peptone dextrose (YPD) medium at 30°C. Yeast strains were obtained from the EUROSCARF collection.

Escherichia coli strain DH5α was grown on Luria-Bertani (LB) medium containing antibiotics, at 37°C. Agrobacterium tumefaciens strain GV3101 harbouring binary vector constructs was grown on antibiotic-containing LB media at 28°C.

Two tomato genotypes were used in this study: *Solanum lycopersicum* MM and *Solanum habrochaites* cv. LA1777. LA1777 and *On*-Lz constitute an incompatible interaction, whereas MM is highly susceptible to *On*-Lz. Tomato seeds were surface sterilized with 3% sodium hypochlorite for 3 min and immediately rinsed with sterile distilled water three times, as previously described (Sun et al., 2018). Seeds were germinated in vermiculite and grown in a growth chamber for 7 days under the following environmental conditions: 25 ± 0.5°C, 95–100% relative humidity (RH), and continuous illumination of 3,500 lux provided by fluorescent lamps. Once the cotyledon leaves had unfolded, the plants were transplanted to soil in 15 cm pots and grown in a temperature-controlled glasshouse (25 ± 3°C) for 1 month before they were used for pathogen inoculation experiments.

N. benthamiana plants were grown in a growth chamber at 20°C under a 16-hr light/8-hr dark cycle with 60% relative humidity and a light intensity of 120-mmol photons m^{-2} s^{-1}.

Arabidopsis thaliana seeds included ecotype Columbia-0 (WT Col-0) and the T-DNA insertion mutant *arpc3* (SALK_099449) were obtained from the Arabidopsis Biological Resource Center (ABRC; The Ohio State University). Seeds were sterilized in 50% bleach (v/v) containing 0.05% Triton X-100 (v/v) for 10 min, rinsed five times with sterile water, and incubated at 4°C for 3 days. For germination, 10 seeds were transferred to 1 ml ½-strength Murashige–Skoog (MS) liquid medium (MS salt supplemented with 0.5% sucrose [w/v], pH 5.5 [pH adjusted to 5.7 by KOH, pH 5.5 after autoclaving], in each well of a six-well plate; Wu et al., 2014). Germination and growth took place in a growth chamber at 21°C and 19°C during the 8 hr day and 16 hr night periods, respectively. Relative humidity was 70% and light intensity was 100 W m^{-2}.

4.2 | Sequencing and phylogenetic analysis of ShARPC3

Tomato ARPC3 (Accession number Solyc07g007630) amino acid sequence was used as a query in a TBLASTN program against the SGN Tomato Combined database (http://

solgenomics.net/tools/blast/), in a BLASTP program against an Arabidopsis protein database (http://www.arabidopsis.org/Blast/index.jsp), or GenBank using BLASTN (http://blast.ncbi.nlm.nih.gov/Blast.cgi) to identify homologous sequences. Conserved and homologous tomato expressed sequence tag (EST) sequences were extracted and assembled. The cDNA sequence of *ShARPC3* was analysed in silico using BLAST and the Open Reading Frame (ORF) Finder software in NCBI (http://www.ncbi.nlm.nih.gov/gorf/gorf.html). Multiple sequence alignments were performed using CLUSTALX2.0 (DNASTAR; http://www.dnastar.com/) and DNAMAN6.0 (Lynnon BioSoft). Phylogenetic analysis was performed using the MEGA software package (v.6.0; http://www.megasoftware.net/) using the neighbour-joining method. The protein domain predictions were assigned on the basis of analysis using the SMART database (http://smart.embl-heidelberg.de) and RCSB PDB protein databank (https://www.rcsb.org/).

Predicted protein-protein interactions between tomato ARPC3 and other tomato proteins were determined using STRING (http://string-db.org/; Franceschini et al., 2013). To reduce the number of hits (i.e., potential false positives), the minimum required interaction score was set to the highest confidence interval (0.900), and the maximum number of interactors was set to not more than 10 interactors. The subcellular localization of *Sh*ARPC3 protein was predicted from the amino acid sequence using Procomp (v.9.0; http://linux1.softberry.com/berry.phtml).

4.3 | Plasmid construction

The coding sequence (cDNAs) of *ShARPC3* was amplified from reverse-transcribed RNA and cloned using gene-specific DNA primers (Table S1). For subcellular localization analysis of *Sh*ARPC3, the full-length cDNA of *ShARPC3* was cloned into the pCaMV35S::*GFP* vector via *Bam*HI digestion and ligation. For transient expression assays in tobacco, the *ShARPC3* ORF was amplified with DNA primers (Table S1) designed to introduce a *Sal*I restriction enzyme site. The amplified product was digested and ligated into the *Sal*I site of the binary vector pGR106 using SmartSeamless Cloning kit. The VIGS vectors were constructed using tobacco rattle virus (TRV1 and TRV2) according to the methods of Dong, Burch-Smith, Liu, Mamillapalli, and Dinesh-Kumar (2007). The target sequence for *ShARPC3* VIGS started from the non-coding 5′ region and included 427 nucleotides of the *ShARPC3* ORF. Selected gene fragments of *ShARPC3* were amplified by PCR from tomato cDNA using the primers *Bam*HI with restriction enzyme site (Table S1). The resultant PCR products were ligated into the TRV2 vector using the SmartSeamless Cloning Kit, yielding TRV2:*ShARPC3*. DNA constructs were extracted using the plasmid extracting kit from Qiagen (Shanghai, China) and sequenced to confirm the presence of the intended inserts. For the Arabidopsis *arpc3* mutant complementation assays, PCR-amplified cDNAs of *ShARPC3* (Table S1) was subcloned with *Bam*HI digestion site and inserted between 35S promoter and NOS terminator sequences of the binary vector pCAMBIA3301-*ShARPC3* using the SmartSeamless Cloning Kit. For yeast *arc18* mutant complementation assays, PDR195-*ShARPC3* expression constructs were created by cloning PCR-amplified *ShARPC3* cDNA into the *Not*I restriction enzyme (Promega, Madison, WI, USA) site of the binary vector PDR195 using the SmartSeamless Cloning Kit (Jieyi Biotech, Shanghai, China).

4.4 | Subcellular localization analysis

Protoplast isolation from tomato leaves was performed as previously described (Yu et al., 2015), with minor modifications. In brief, leaves of ~8-week-old tomato plants were used for subcellular localization analyses. Leaves were dissected into 0.5–1-mm strips using a razor blade and incubated at room temperature (~22°C) in 1% cellulase R10 (Yakult Pharmaceutical Ind. Co., Ltd., Tokyo, Japan), 0.25% macerozyme R10 (Yakult Pharmaceutical Ind. Co., Ltd.), 0.4 M mannitol, 20 mM KCl, 10 mM $CaCl_2$, and 20 mM 2-(N-morpholino) ethanesulfonic acid (MES) for 3–4 hr, with shaking at 40–50 rpm. Following incubation at room temperature, the protoplast preparation was filtered through a metal sieve, and the eluate was centrifuged at 100 *g* for 5 min. Pelleted protoplasts were suspended in 5 ml of W5 solution (154 mM NaCl, 125 mM $CaCl_2$, 5 mM KCl, and 2 mM MES/KOH; pH 5.7) and centrifuged for 5 min at 100 *g*. The protoplasts were transferred to a tube containing 5 ml of the W5 solution. The protoplasts were pelleted again by centrifugation at 100 *g* for 5 min and resuspended in 5 ml of the W5 solution. Protoplasts were incubated on ice for 30 min and then resuspended in 5 ml of MMg buffer (400 mM mannitol, 15 mM $MgCl_2$, and 4 mM MES/KOH; pH 5.7). For cotransformation, 10 μg of recombinant plasmid pCaMV35S:*ShARPC3-GFP*, or empty vector pCaMV35S:*GFP* was added to 100 μl of the protoplast suspension. An equal volume of 40% (w/v) PEG3350, freshly prepared with 0.1 M $CaCl_2$ and 0.8 M mannitol solution, was added. Then, the mixture was incubated at room temperature for 30 min. After incubation, the mixture was diluted with 500 μl of the W5 solution. The solution containing the protoplasts was gently mixed and the protoplasts were pelleted by centrifugation at 100 *g* for 5 min. Protoplasts were washed twice using the W5 solution, gently resuspended in 1 ml of W5 solution, and incubated in 12-well plates at room temperature for 18–36 hr in the dark. GFP fluorescence was detected using an Olympus FV1000 laser confocal microscope equipped with a 488 nm filter. The experiment was repeated three times.

4.5 | Agrobacterium-mediated transient expression in *N. benthamiana*

The *ShARPC3* gene was amplified using combinations of primers for the PVX (pGR106) assay (Lu et al., 2003). Recombinant plasmid pGR106-*ShARPC3* or pGR106-*GFP* prepared from *E. coli* DH5α was transformed into *A. tumefaciens* strain GV3101 via electroporation. Transformants were grown at 28°C with 50 μg ml^{-1} of each of rifampicin and kanamycin until cultures reached stationary growth phase. Cultures of Agrobacterium transformed with pGR106-*GFP* or pGR106-*ShARPC3* were centrifuged and the resultant bacterial pellets resuspended in infiltration buffer (10 mM $MgCl_2$, 150 μM acetosyringone, 10 mM MES pH 5.6) to a final OD 600 nm of 0.1. After incubation for 2–3 hr in the dark, *A. tumefaciens* cells carrying *ShARPC3*, *GFP*, or buffer were infiltrated. After 24 hr, the same infiltration site was challenged with *A. tumefaciens* cells carrying the *BAX* gene. BAX, a death-promoting member of the Bcl-2 family of proteins, triggered cell death when expressed in plants (Lacomme & Santa, 1999). *A. tumefaciens* strains carrying *GFP* gene alone were infiltrated in parallel as negative control. Symptom development was monitored visually 5 to 7 days after infiltration. This experiment was repeated three times with each assay consisting of three plants each, with three leaves inoculated.

4.6 | TRV2-mediated silencing of ShARPC3 in tomato

VIGS TRV1 and TRV2-*ShARPC3* were introduced into *A. tumefaciens* strain GV3101 by heat shock. A total of 5 ml of an overnight culture was grown at 28°C in the appropriate antibiotic selection medium in a 15-ml glass tube for 24 hr, after which time cultures were spun down and cells were resuspended in infiltration medium (10 mM MES, 10 mM $MgCl_2$, 200 μM acetosyringone), adjusted to an OD 600 nm of 1.0, and incubated at room temperature for 3 hr. Agroinfiltration was performed as previously described (Liu, Schiff, Marathe, & Dinesh-Kumar, 2002). The first and second leaves of four-leaf stage LA1777 plants were infiltrated with a 1:1 mixture of TRV1 and TRV2-*ShARPC3* fragment for the clone. The empty vector TRV2 was used as negative control. To monitor silencing efficiency, plants were inoculated in parallel with TRV2 expressing phytoene desaturase (i.e., TRV2:*ShPDS*; accession number NM_001247166). Following virus inoculation, seedlings were transferred to an environmentally controlled growth chamber (25°C, 16-hr light/8-hr dark photoperiod). Photobleaching symptoms in the PDS control plants were observed ~30 days after virus inoculation. The fourth leaves of plants were inoculated with *On*-Lz; sampled at 6, 18, 24, 48, and 72 hpi; and processed for histological observation. Five plants were inoculated per trial, and three biological replicates were performed.

4.7 | *A. thaliana* transgenic complementation analysis

Arabidopsis genomic DNA preparation was performed as previously described (Qian et al., 2001). SALK_099449 T-DNA insertions in the *AtARPC3* gene were confirmed by PCR and sequencing using the following DNA primers: SALK_099449LP (5′-AAGGTAGAGGCTCAAACGCTC-3′), SALK_099449RP (5′-AGAATCGCCACCTTTAGCTTC-3′), and the T-DNA-specific primer LBb1.3 (5′-ATTTTGCCGATTTCGGAAC-3′). The complete ORF of *ShARPC3* was cloned into the binary expression vector pCAMBIA3301 carrying CaMV35S promoter. pCAMBIA3301-*ShARPC3* was transformed into *A. tumefaciens* GV3101 and was introduced into WT Col-0 and *arpc3* by the floral dip method (Clough & Bent, 1998). Transgenic T1 plants were selected with kanamycin (25 μg ml^{-1}) on ½-strength MS medium containing 1% Phytoagar. After 2 weeks, kanamycin-resistant seedlings were transplanted to soil. Three- month-old kanamycin-resistant T2 plants from individual T1 lines were pooled (three or four individuals per sample) and assayed for resistance to *On*-Lz as described below. Kanamycin-resistant siblings of these T2 individuals were confirmed as transgenic by PCR using the following DNA primers: (LP-5′-CGGTGTTCTCTCCAAATGAAATGAACTT-3′ and RP-5′-AATTGAGACTTTTCAACAAAGGGTAATA-3′) specific to the 35S promoter of the transgene expression construct. The leaves of plants were inoculated with *On*-Lz; sampled at 6, 18, 24, 48, and 72 hpi; and processed for histological observation. Five plants were inoculated per trial and three biological replicates were performed.

4.8 | Quantitative real-time PCR analysis (qRT-PCR)

To evaluate the expression levels of *ShARPC3* in response to *On*-Lz infection, MM, and LA1777 plant leaves were harvested at 0, 12, 18, 24, 36, 48, 72, and 96 hpi, respectively. For TRV2-mediated silencing of *ShARPC3* assay efficiency the relative expression of *PR1B1* (*PR1*), *Glucanase A* (*PR2*), *Glucanase B* (*PR2-like*), *Chitinase 3* (*PR3*), and *Chitinase 9*

(*PR3-like*; SA pathway-specific gene expression markers; Schenk et al., 2000) were assessed by sampling the fourth leaves of *SlARPC3*-silenced tomato plants at 0, 24, 48, and 72 hpi following infection with *On*-Lz. The *GAPDH* gene was used as the internal control for qRT-PCR analysis (Chalupowicz et al., 2010). DNA primers for qRT-PCR are listed in Table S2. For Arabidopsis transgenic complementation assays, leaves were inoculated with *On*-Lz; sampled at 0, 24, 48, and 72 hpi; and processed for RNA isolation (below). The *UBQ10* gene was used as the control for qRT-PCR reactions. DNA primers used for qRT-PCR analysis are listed in Table S3. Total RNA was prepared using the BIOZOL total RNA extraction kit (Gentaur, Belgium) following the manufacturer's instructions. RNA integrity was evaluated by gel electrophoresis, and the RNA concentration was determined using a Qubit 2.0 Fluorometer (Life Technologies, Thermo Fisher, Waltham, MA, USA). Total RNA (1 μg) was used for first strand cDNA synthesis using the single strand cDNA synthesis kit (GeneCopoeia, Rockville, MD, USA) with oligo $(dT)_{18}$ primer (MBI Fermentas/Thermo Fisher, Waltham, MA, USA).

The IQ™5 Real-Time PCR System (BioRad, Hercules, CA, USA) was employed for quantitative PCR amplification. For real-time PCR reactions, 1 μl total cDNA was added to a 20 μl PCR reaction mixture containing 10 μl of 2X ultra SYBR Mixture (CWBIO, Beijing, China), 0.4 μl of each primer, 2 μl template, and 7.2 μl of water. qRT-PCR conditions were as follows: denaturing at 95°C for 10 min, followed by 40 cycles of 15 s at 95°C, 30 s at 55°C, and 30 s at 72°C. Each reaction included a nontemplate control. All analyses were performed in biological triplicate. Relative transcript quantification was calculated by the comparative $2^{-\Delta\Delta CT}$ method (Livak & Schmittgen, 2001). Statistical analysis was performed using two-tailed analysis of variance (ANOVA) with the SPSS 17.0 program (IBM SPSS Statistics; https://www.ibm.com/products/spss-statistics). A value of $P < .05$ indicates a significant difference between groups.

4.9 | Pathogen inoculation, phenotypic, and histological observations

The fresh *On*-Lz conidia were collected from infected plant leaves with sterile water. Four-week plants were used for inoculation by spraying a spore suspension of 5×10^4 conidia/ml on the whole plants for the histological study. The infection phenotypes of tomato and *A. thaliana* leaves were observed at 7 dpi. For VIGS assay, disease index (DI) was evaluated at 7–14 dpi (Sun et al., 2017). Disease severity was scored according to the following: 0 = no diseased leaves; 1 = 0–5% of leaves having lesions; 3 = leaves with infection lesions up to 6–10%; 5 = leaves with infection lesions up to 11–20%; 7 = leaves with infection lesions up to 21–40%; and 9 = leaves with infection lesions up to 41–100%.

Disease index was calculated using the following equation:

Disease index (DI) = [Σ (number of diseased plant leaves at a given disease severity × the disease severity)/(total plant leaves analysed × 9)] × 100%. An average DI was calculated at three independent times for each infected plant.

To quantify fungal growth, the number of conidiophores per colony was counted at 7 dpi as previously described (Consonni et al., 2006). At least 25 colonies were counted for each genotype in each experiment. Infection assays and disease severity evaluations were

repeated three times. To quantify the accumulation of H_2O_2 (H_2O_2 production rate = H_2O_2 numbers per 100 penetration sites) and the induction of HR cell death (HR production rate = HR numbers per 100 penetration sites) during *On*-Lz infection, 3,3-diaminobenzidine (DAB) and trypan blue staining were performed following the method of Thordal-Christensen, Zhang, Wei, and Collinge (1997). All microscopic examinations were performed using a Nikon Eclipse 80i microscope equipped with DIC (Nikon Corporation, Tokyo, Japan). At least 50 penetration sites on each of four-leaf samples were observed at each time point. Standard errors of deviation were calculated using Microsoft Excel. Statistical significance was assessed by a Student's *t* test ($P < .05$) using SPSS software.

4.10 | Quantification of phytohormone content

Tomato leaves from VIGS experiments were used for phytohormone analysis. Leaves were separately collected at 0, 1, 3, 6, 12, and 24 hr after inoculation with *On*-Lz according to Gong et al. (2017). Three biological replicates were performed. Standard errors of deviation were calculated using Microsoft Excel. Statistical significance was assessed by a Student's *t* test ($P < .05$) using SPSS software.

4.11 | Yeast mutant complementation assay

The complete ORF of *ShARPC3* was cloned into pDR195 (Addgene, plasmid #36028). The transformed cell (Δ*arc18* + *ShARPC3*) was obtained by transforming the reconstructed vector (pDR195- *ShARPC3*) into the mutant strain Y06714. The transformed cell containing the empty vector pDR195 (Δ*arc18* + empty) was used as a control. To investigate yeast cell survival under stress, transformed cells (initial optical density [OD] of 0.6–1.0 at 600 nm) were cultured in yeast medium. The concentration of pDR195 (Δ*arc18* + empty) and pDR195-*ShARPC3* (Δ*arc18* + *ShARPC3*) transformed cells, as well as WT yeast cells (BY4741) were serially diluted to 10^7, 10^6, 10^5, 10^4, and 10^3 (cells ml^{-1}) using an Olympus BX-51 microscope (Olympus) coupled with a blood counting chamber. This experiment was repeated three times.

Supplementary Material

Refer to Web version on PubMed Central for supplementary material.

ACKNOWLEDGMENTS

The research presented herein was supported by the National Natural Science Foundation of China (Grant 31571960), Key Industrial Chain Projects of Shaanxi (2019ZDLNY03-07), Northwest A&F University extension Project (2018-10), and the 111 Project from the Ministry of Education of China (Grant B07049). Research in the laboratory of B.D. is supported by the U.S. National Science Foundation (IOS-1557437) and the National Institutes of General Medical Sciences (1R01GM125743).

REFERENCES

Bai Y, Huang CC, Van Der Hulst R, Meijer-Dekens F, & Bonnema G (2003). Lindhout P QTLs for tomato powdery mildew resistance (*Oidium lycopersici*) in *Lycopersicon parviflorum* G1.1601 co-localize with two qualitative powdery mildew resistance genes. Molecular Plant-Microbe Interactions, 16, 169–176. 10.1094/MPMI.2003.16.2.169 [PubMed: 12575751]

Bai Y, Van Der Hulst R, Bonnema G, Marcel TC, Meijer-Dekens F, Niks R, & Lindhout P (2005). Tomato defense to *Oidium neolycopersici*: Dominant *Ol* genes confer isolate-dependent resistance

via a different mechanism than recessive *ol-2*. Molecular Plant-Microbe Interactions, 18, 354–362. 10.1094/MPMI-18-0354 [PubMed: 15828687]

Campellone KG, & Welch MD (2010). A nucleator arms race: Cellular control of actin assembly. Nature Reviews Molecular Cell Biology, 11, 237–251. 10.1038/nrm2867 [PubMed: 20237478]

Chalupowicz L, Cohen-Kandli M, Dror O, Eichenlaub R, Gartemann KH, Sessa G, … Manulis-Sasson S (2010). Sequential expression of bacterial virulence and plant defense genes during infection of tomato with *Clavibacter michiganensis* subsp. *michiganensis*. Phytopathology, 100, 252–261. 10.1094/PHYTO-100-3-0252 [PubMed: 20128699]

Chesarone MA, & Goode BL (2009). Actin nucleation and elongation factors: Mechanisms and interplay. Current Opinion in Cell Biology, 21, 28–37. 10.1016/j.ceb.2008.12.001 [PubMed: 19168341]

Chisholm S, Coaker G, Day B, & Staskawicz BJ (2006). Host-microbe interactions: Shaping the evolution of the plant immune response. Cell, 124, 1–12.

Ciccarese F, Amenduni M, Ambrico A, & Cirulli M (2000). The resistance to *Oidium lycoeprsici* conferred by *ol-2* gene in tomato. Acta Physiologiae Plantarum, 22, 266.

Clough SJ, & Bent AF (1998). Floral dip: A simplified method for Agrobacterium-mediated transformation of *Arabidopsis thaliana*. The Plant Journal, 16, 735–743. 10.1046/j.1365-313x.1998.00343.x [PubMed: 10069079]

Consonni C, Humphry ME, Hartmann HA, Livaja M, Durner J, Westphal L, … Panstruga R (2006). Conserved requirement for a plant host cell protein in powdery mildew pathogenesis. Nature Genetics, 38, 716–720. 10.1038/ng1806 [PubMed: 16732289]

Day B, Henty J, Porter K, & Staiger C (2011). The pathogen-actin connection: A platform for defense signaling in plants. Annual Review of Phytopathology, 49, 483–506. 10.1146/annurev-phyto-072910-095426

Dong YY, Burch-Smith TM, Liu YL, Mamillapalli P, & Dinesh-Kumar SP (2007). A ligation-independent cloning tobacco rattle virus vector for high-throughput virus-induced gene silencing identifies roles for NBMADS4–1 and −2 in floral development. Plant Physiology, 145, 1161–1170. 10.1104/pp.107.107391 [PubMed: 17932306]

Franceschini A, Simonovic M, Roth A, Von Mering C, Szklarczyk D, Pletscher-Frankild S, … Bork P (2013). STRING v9. 1: Protein-protein interaction networks, with increased coverage and integration. Nucleic Acids Research, 41, D808–D815. 10.1093/nar/gks1094 [PubMed: 23203871]

Fu Y, Duan X, Tang C, Li X, Voegele RT, Wang X, … Kang Z (2014). *Ta*ADF7, an actin-depolymerizing factor, contributes to wheat resistance against *Puccinia striiformis* f. sp. *tritici*. The Plant Journal, 78, 16–30. 10.1111/tpj.12457 [PubMed: 24635700]

Gong C, Liu Y, Liu SY, Cheng MZ, Zhang Y, Wang RH, … Wang AX (2017). Analysis of *Clonostachys rosea*-induced resistance to grey mould disease and identification of the key proteins induced in tomato fruit. Postharvest Biology and Technology, 123, 83–93. 10.1016/j.postharvbio.2016.08.004

Gourlay CW, & Ayscough KR (2005). The actin cytoskeleton: A key regulator of apoptosis and ageing. Nature Reviews Molecular Cell Biology, 6, 583–589. 10.1038/nrm1682 [PubMed: 16072039]

Henty-Ridilla JL, Shimono M, Li J, Chang J, Day B, & Staiger CJ (2013). The plant actin cytoskeleton responds to signals from microbe-associated molecular patterns. PLoS Pathogens, 9, e1003290 10.1371/journal.ppat.1003290 [PubMed: 23593000]

Huot J, Houle F, Rousseau S, Deschesnes RG, Shah GM, & Landry J (1998). SAPK2/p38-dependent F-actin reorganization regulates early membrane blebbing during stress-induced apoptosis. Journal of Cell Biology, 143, 1361–1373. 10.1083/jcb.143.5.1361

Jaffe AB, & Hall A (2005). Rho GTPases: Biochemistry and biology. Annual Review of Cell and Developmental Biology, 21, 247–269. 10.1146/annurev.cellbio.21.020604.150721

Jones H, Whipps JM, & Guu SJ (2001). The tomato powdery mildew fungus *Oidium neolycopersici*. Molecular Plant Pathology, 2, 303–309. 10.1046/j.1464-6722.2001.00084.x [PubMed: 20573019]

Jones JD, & Dangl JL (2006). The plant immune system. Nature, 444, 323–329. 10.1038/nature05286 [PubMed: 17108957]

Kim H, Park M, Kim SJ, & Hwang I (2005). Actin filaments play a critical role in vacuolar trafficking at the Golgi complex in plant cells. Plant Cell, 17, 888–902. 10.1105/tpc.104.028829 [PubMed: 15722471]

Kobayashi I, Kobayashi Y, & Hardham AR (1994). Dynamic reorganization of microtubules and microfilaments in flax cells during the resistance response to flax rust infection. Planta, 195, 237–247.

Kotchoni SO, Zakharova T, Mallery EL, Le J, El-Assal SE, & Szymanski DB (2009). The association of the Arabidopsis actin-related protein2/3 complex with cell membranes is linked to its assembly status but not its activation. Plant Physiology, 151, 2095–2109. 10.1104/pp.109.143859 [PubMed: 19801398]

Lacomme C, & Santa CS (1999). Bax-induced cell death in tobacco is similar to the hypersensitive response. Proceedings of the National Academy of Sciences, 96, 7956–7961. 10.1073/pnas.96.14.7956

Lan A, Huang J, Zhao W, Peng Y, Chen Z, & Kang D (2013). A salicylic acid-induced rice (*Oryza sativa* L.) transcription factor *Os*WRKY77 is involved in disease resistance of *Arabidopsis thaliana*. Plant Biology, 15, 452–461. 10.1111/j.1438-8677.2012.00664.x [PubMed: 23061987]

Lebeda A, Mieslerová B, Petřivalský M, Luhová L, Špundová M, Sedlářová M, … Pink DAC (2014). Resistance mechanisms of wild tomato germplasm to infection of *Oidium neolycopersici*. European Journal of Plant Pathology, 138(SI), 569–596. 10.1007/s10658-013-0307-3

Li CW, Bai YL, Jacobsen E, Visser R, Lindhout P, & Bonnema G (2006). Tomato defense to the powdery mildew fungus: Differences in expression of genes in susceptible, monogenic- and polygenic resistance responses are mainly in timing. Plant Molecular Biology, 62, 127–140. 10.1007/s11103-006-9008-z [PubMed: 16900321]

Li L, & Zou Y (2017). Induction of disease resistance by salicylic acid and calcium ion against *Botrytis cinerea* in tomato (*Lycopersicon esculentum*). Emirates Journal of Food Agriculture, 29, 78–82. 10.9755/ejfa.2016-10-1515

Li P, & Day B (2019). Battlefield cytoskeleton: Cytoskeletal regulation and pathogen targeting of plant immunity. Mol Plant-Microbe Interact., 32, 25–34. 10.1094/MPMI-07-18-0195-FI [PubMed: 30355064]

Lindhout P, Pet G, & van der Beek H (1994). Screening wild Lycopersicon species for resistance to powdery mildew (*Oidium lycopersicum*). Euphytica, 72, 43–49.

Lindhout P, van der Beek H, & Pet G (1994). Wild *Lycopersicon* species as sources for resistance to powdery mildew (*Oidium lycopersicum*): Mapping of resistance gene *Ol-1* on chromosome 6 of *Lycopersicon hirsutum*. Acta Horticulturae, (376), 387–394.

Liu YL, Schiff M, Marathe R, & Dinesh-Kumar SP (2002). Tobacco *Rar1*, *EDS1* and *NPR1/NIM1* like genes are required for N-mediated resistance to tobacco mosaic virus. The Plant Journal, 30, 415–429. 10.1046/j.1365-313X.2002.01297.x [PubMed: 12028572]

Livak KJ, & Schmittgen TD (2001). Analysis of relative gene expression data using real-time quantitative PCR and the $2^{-\Delta\Delta CT}$ method. Methods, 25, 402–408. 10.1006/meth.2001.1262 [PubMed: 11846609]

Lu R, Malcuit I, Moffett P, Ruiz MT, Peart J, Wu AJ, … Baulcombe DC (2003). High throughput virus-induced gene silencing implicates heat shock protein 90 in plant disease resistance. EMBO Journal, 22, 5690–5699. 10.1093/emboj/cdg546

Machesky LM, Atkinson SJ, Ampe C, Vandekerckhove J, & Pollard TD (1994). Purification of a cortical complex containing two unconventional actins from *Acanthamoeba* by affinity chromatography on profilin-agarose. Journal of Cell Biology, 127, 107–116. 10.1083/jcb.127.1.107

Machesky LM, Mullins RD, Higgs HN, Kaiser DA, Blanchoin L, May RC, … Pollard TD (1999). Scar, a WASP-related protein, activates nucleation of actin filaments by the Arp2/3 complex. Proceedings of the National Academy of Science of the United States of America, 96, 3739–3744. 10.1073/pnas.96.7.3739

Maisch J, Fiserova J, Fischer L, & Nick P (2009). Tobacco Arp3 is localized to actin-nucleating sites *in vivo*. Journal of Experimental Botany, 60, 603–614. 10.1093/jxb/ern307 [PubMed: 19129161]

Marcel TC, Gorguet B, Ta MT, Kohutova Z, Vels A, & Niks RE (2008). Isolate specificity of quantitative trait loci for partial resistance of barley to *Puccinia hordei* confirmed in mapping populations and near-isogenic lines. New Phytologist, 177, 743–755. 10.1111/j.1469-8137.2007.02298.x

Mathur J, & Hülskamp M (2002). Microtubules and microfilaments in cell morphogenesis in higher plants. Current Biology, 12, R669–R676. 10.1016/S0960-9822(02)01164-8 [PubMed: 12361589]

Mathur J, Mathur N, Kernebeck B, & Hülskamp M (2003). Mutations in actin-related proteins 2 and 3 affect cell shape development in Arabidopsis. The Plant Cell, 15, 1632–1645. 10.1105/tpc.011676 [PubMed: 12837952]

Mathur J, Mathur N, Kirik V, Kernebeck B, Srinivas BP, & Hulskamp M (2003). *Arabidopsis*, *CROOKED* encodes for the smallest subunit of the ARP2/3 complex and controls cell shape by region specific fine F-actin formation. Development, 130, 3137–3146. 10.1242/dev.00549 [PubMed: 12783786]

Molitor A, Zajic D, Voll LM, Pons KHJ, Samans B, Kogel KH, & Waller F (2011). Barley leaf transcriptome and metabolite analysis reveals new aspects of compatibility and *Piriformospora indica*-mediated systemic induced resistance to powdery mildew. Molecular Plant-Microbe Interactions, 24, 1427–1439. 10.1094/MPMI-06-11-0177 [PubMed: 21830949]

Mouekouba LD, Zhang L, Guan X, Chen X, Chen H, Zhang J, … Wang A (2014). Analysis of *Clonostachys rosea*-induced resistance to tomato gray mold disease in tomato leaves. PLoS One, 9, e102690 10.1371/journal.pone.0102690 [PubMed: 25061981]

Nakajima M, & Akutsu K (2014). Virulence factors of *Botrytis cinerea*. Journal of General Plant Pathology, 80, 15–23. 10.1007/s10327-013-0492-0

Opalski KS, Schultheiss H, Kogel KH, & Hückelhoven R (2005). The receptor-like MLO protein and the RAC/ROP family G-protein RACB modulate actin reorganization in barley attacked by the biotrophic powdery mildew fungus *Blumeria graminis* f.sp. *hordei*. The Plant Journal, 41, 291–303. 10.1111/j.1365-313X.2004.02292.x [PubMed: 15634205]

Pantaloni D, le Clainche C, & Carlier MF (2001). Mechanism of actin-based motility. Science, 292, 1502–1506. 10.1126/science.1059975 [PubMed: 11379633]

Pei DL, Ma HZ, Zhang Y, Ma YS, Wang WJ, Geng HX, … Li CW (2011). Silencing a putative cytosolic NADP-malic enzyme gene compromised tomato resistance to *Oidium neolycopersici*. Life Science Journal, 8, 652–657.

Peterhänsel C, Freialdenhoven A, Kurth J, Kolsch R, & Schulze-Lefert P (1997). Interaction analyses of genes required for resistance responses to powdery mildew in barley reveal distinct pathways leading to leaf cell death. The Plant Cell, 9, 1397–1409. 10.1105/tpc.9.8.1397 [PubMed: 12237388]

Pollard TD, Blanchoin L, & Mullins RD (2000). Molecular mechanisms controlling actin filament dynamics in nonmuscle cells. Annual Review of Biophysics and Biomolecular Structure, 29, 545–576.

Pollard TD, & Borisy GG (2003). Cellular motility driven by assembly and disassembly of actin filaments. Cell, 112, 453–465. [PubMed: 12600310]

Poraty-Gavra L, Zimmermann P, Haigis S, Bednarek P, Hazak O, Stelmakh OR, … Yalovsky S (2013). The Arabidopsis Rho of plants GTPase AtROP6 functions in developmental and pathogen response pathways. Plant Physiology, 161, 1172–1188. 10.1104/pp.112.213165 [PubMed: 23319551]

Porter K, & Day B (2015). From filaments to function: The role of the plant actin cytoskeleton in pathogen perception, signaling, and immunity. Journal of Integrative Plant Biology, 58, 299–311. [PubMed: 26514830]

Qi T, Wang J, Sun Q, Day B, Guo J, & Ma Q (2017). *TaARPC3*, contributes to wheat resistance against the stripe rust fungus. Frontiers in Plant Science, 8 10.3389/fpls.2017.01245

Qian Q, Li YH, Zeng D, Teng S, Wang Z, Li X, … Li J (2001). Isolation and genetic characterization of a fragile plant mutant rice. (*Oryza sativa L.*). Chinese Science Bulletin, 46, 2082–2085. 10.1007/BF02901137

Roberts P, Momol T, & Pernezny K (2002). Powdery mildew on tomato, document PP-191 of Plant Pathology Department, Florida Cooperative Extension Service, Institute of Food and Agricultural Sciences, University of Florida.

Schenk PM, Kazan K, Wilson I, Anderson JP, Richmond T, Somerville SC, & Manners JM (2000). Coordinated plant defense responses in Arabidopsis revealed by microarray analysis. Proceedings of the National Academy of Sciences, 97, 11655–11660. 10.1073/pnas.97.21.11655

Shimono M, Higaki T, Kaku H, Shibuya N, Hasezawa S, & Day B (2016). Quantitative evaluation of stomatal cytoskeletal patterns during the activation of immune signaling in *Arabidopsis thaliana*. PLoS One, 11, e0159291 10.1371/journal.pone.0159291 [PubMed: 27415815]

Shimono M, Lu Y, Porter K, Kvitko B, Creason A, Henty-Ridilla J, … Day B (2016). The *Pseudomonas syringae* type III effector HopG1 induces actin filament remodeling in Arabidopsis in association with disease symptom development. Plant Physiology, 171, 2239–2255. 10.1104/pp.16.01593 [PubMed: 27217495]

Sparkes I, Runions J, Hawes C, & Griffing L (2009). Movement and remodeling of the endoplasmic reticulum in non-dividing cells of tobacco leaves. The Plant Cell, 21, 3937–3949. 10.1105/tpc.109.072249 [PubMed: 20040535]

Sun GZ, Wang H, Shi BB, Shangguan NN, Wang Y, & Ma Q (2017). Control efficiency and expressions of resistance genes in tomato plants treated with ε-poly-l-lysine against *Botrytis cinerea*. Pesticide Biochemistry and Physiology, 143, 191–198. 10.1016/j.pestbp.2017.07.007 [PubMed: 29183591]

Sun GZ, Yang QC, Zhang AC, Guo J, Liu XJ, Wang Y, & Ma Q (2018). Synergistic effect of the combined bio-fungicides ε-poly-L-lysine and chitooligosaccharide in controlling grey mould (*Botrytis cinerea*) in tomatoes. International Journal of Food Microbiology, 276, 46–53. 10.1016/j.ijfoodmicro.2018.04.006 [PubMed: 29656220]

Takenawa T, & Miki H (2001). WASP and WAVE family proteins: Key molecules for rapid rearrangement of cortical actin filaments and cell movement. Journal of Cell Science, 114, 1801–1809. [PubMed: 11329366]

Takken FL, Albrecht M, & Tameling WI (2006). Resistance proteins: Molecular switches of plant defence. Current Opinion in Plant Biology, 9, 383–390. 10.1016/j.pbi.2006.05.009 [PubMed: 16713729]

Thordal-Christensen H, Zhang ZG, Wei YD, & Collinge DB (1997). Subcellular localization of H_2O_2 in plants. H_2O_2 accumulation in papillae and hypersensitive response during the barley-powdery mildew interaction. The Plant Journal, 11, 1187–1194. 10.1046/j.1365-313X.1997.11061187.x

Tian M, Chaudhry F, Ruzicka DR, Meagher RB, Staiger CJ, & Day B (2009). *Arabidopsis* actin-depolymerizing factor *AtADF4* mediates defense signal transduction triggered by the *Pseudomonas syringae* effector AvrPphB. Plant Physiology, 150, 815–824. 10.1104/pp.109.137604 [PubMed: 19346440]

Van Verk MC, Pappaioannou D, Neeleman L, Bol JF, & Linthorst HJ (2008). A novel WRKY transcription factor is required for induction of *PR-1a* gene expression by salicylic acid and bacterial elicitors. Plant Physiology, 146, 1983–1995. 10.1104/pp.107.112789 [PubMed: 18263781]

Wang X, Tang C, Zhang G, Li Y, Wang C, Liu B, … Kang ZS (2009). cDNA-AFLP analysis reveals differential gene expression in compatible interaction of wheat challenged with *Puccinia striiformis* f. sp. *tritici*. BMC Genomics, 10, 289 10.1186/1471-2164-10-289 [PubMed: 19566949]

Weaver AM, Young ME, Lee WL, & Cooper JA (2003). Integration of signals to the Arp2/3 complex. Current Opinion in Cell Biology, 15, 23–30. 10.1016/S0955-0674(02)00015-7 [PubMed: 12517700]

Welch MD, Iwamatsu A, & Mitchison TJ (1997). Actin polymerization is induced by Arp2/3 protein complex at the surface of *Listeria monocytogenes*. Nature, 385, 265–268. 10.1038/385265a0 [PubMed: 9000076]

Welch MD, & Mullins RD (2002). Cellular control of actin nucleation. Annual Review of Cell Developmental Biology, 18, 247–288. 10.1146/annurev.cellbio.18.040202.112133

Wu HY, Liu KH, Wang YC, Wu JF, Chiu WL, Chen CY, … Lai EM (2014). AGROBEST: An efficient *Agrobacterium*-mediated transient expression method for versatile gene function analyses in *Arabidopsis* seedlings. Plant Methods, 10, 19 10.1186/1746-4811-10-19 [PubMed: 24987449]

Yokota K, Fukai E, Madsen LH, Jurkiewicz A, Rueda P, Radutoiu S, … Rusek AM (2009). Rearrangement of actin cytoskeleton mediates invasion of *Lotus japonicus* roots by *Mesorhizobium loti*. Plant Cell, 21, 267–284. 10.1105/tpc.108.063693 [PubMed: 19136645]

Yu H, Jiang W, Liu Q, Zhang H, Piao MX, Chen ZD, & Bian MD (2015). Expression pattern and subcellular localization of the ovate protein family in rice. PLoS One, 10, e0118966 10.1371/journal.pone.0118966 [PubMed: 25760462]

Zhang B, Yuan H, Wang J, Huo Y, Shimono M, Day B, & Ma Q (2017). *Ta*ADF4, an actin-depolymerizing factor from wheat, is required for resistance to the stripe rust pathogen *Puccinia striiformis* f. sp. *tritici*. The Plant Journal, 89, 1210–1224. 10.1111/tpj.13459 [PubMed: 27995685]

Zhang R, Xia X, Lindsey K, & Da RP (2012). Functional complementation of *dwf4* mutants of *Arabidopsis* by overexpression of *CYP724A1*. Journal of Plant Physiology, 169, 421–428. 10.1016/j.jplph.2011.10.013 [PubMed: 22196800]

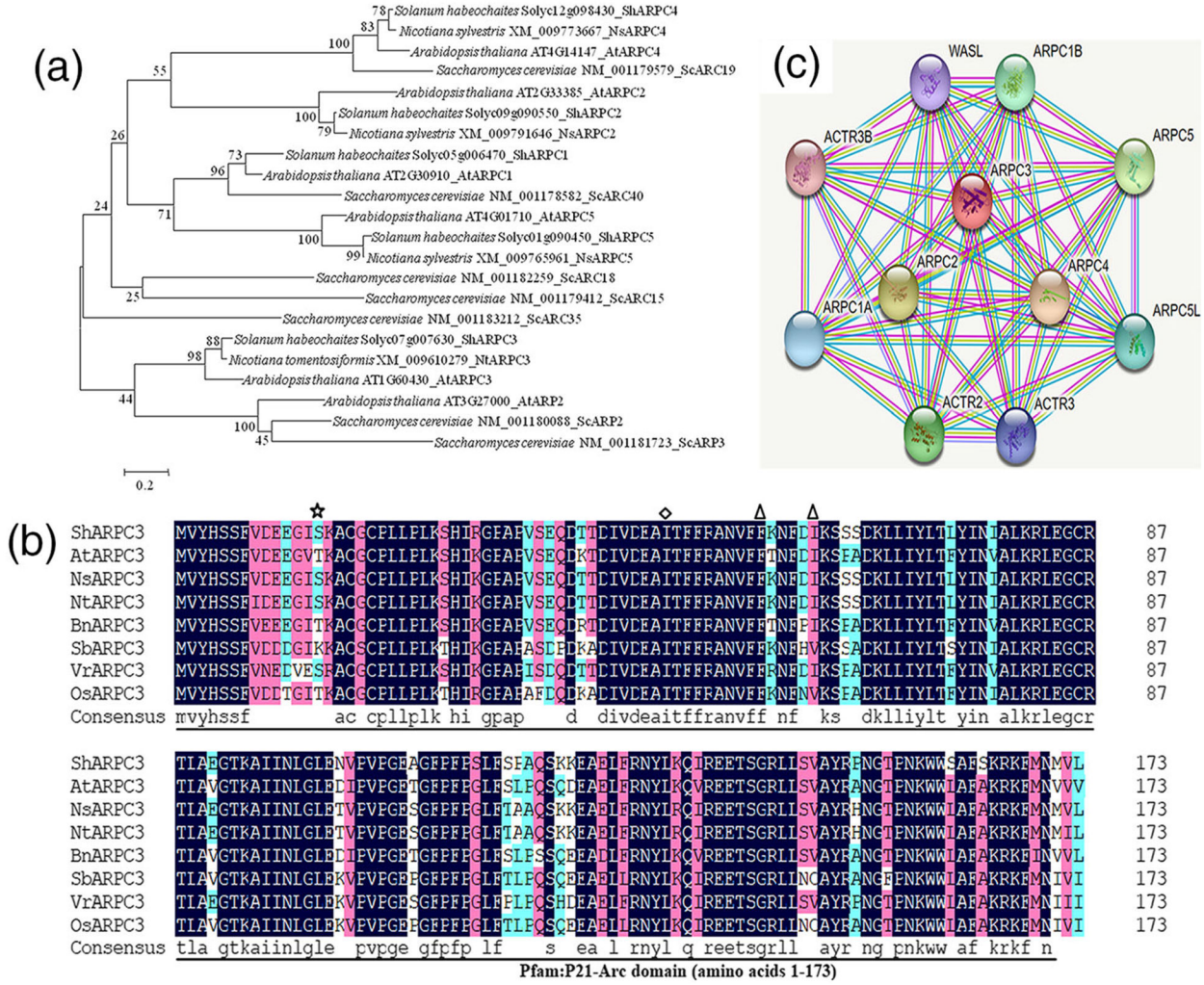

FIGURE 1.

Sequence analysis and predicted interaction network of tomato actin-related protein 2 and 3 (Arp2/3) complex subunit 3 (*Sh*ARPC3). (a) Evolutionary analysis of *Sh*ARPC3. Analysis was conducted using the neighbour-joining method in MEGA6.0. Representative phylogenetic tree of *Sh*ARPC3 and ARP2/3 complex sequences from *Solanum habrochaites* (*Sh*ARP2/3), *Arabidopsis thaliana* (*At*ARP2/3), *Nicotiana sylvestris* (*Ns*ARP2/3), *Nicotiana tomentosiformis* (*Nt*ARP2/3), and *Saccharomyces cerevisiae* (*Sc*ARP2/3). Accession numbers are shown after the gene names. *Sh*ARPC3, encoded by the tomato gene *Solyc07g007630*, is considered to be the tomato ortholog of *Nt*ARPC3 and *At*ARPC3. (b) Multiple protein sequence alignment of *Sh*ARPC3 and characterized members of ARPC3 proteins. Sequence alignment of *Sh*ARPC3 (Solyc07g007630), *At*ARPC3 (AT1G60430), *Ns*ARPC3 (XP_009791878), *Nt*ARPC3 (XP_009608574), *Bn*ARPC3 (XP_022548276), *Sb*ARPC3 (XP_002451839), *Vr*ARPC3 (XP_014510301), and *Os*ARPC3 (XP_015626361). The *ShARPC3* sequence encodes a 174-amino acid protein containing one P21-Arc domain (amino acids 1–173), one glycyl lysine isopeptide (Lys-Gly; interchain with G-Cter in SUMO2)-cross-link site (amino acid 14) is highlighted with asterisk, one phosphotyrosine-modified residue (amino acid 47) is highlighted with a diamond, two N6-acetyllysine-

modified residues (amino acids 56 and 61) are highlighted with a triangle. Amino acid similarity are shown within the Pfam:P21-Arc domain. Black boxes indicate regions of 100% homology, pink boxes indicate ≥75% homology, and cyan boxes highlight ≥50% homology. (c) The network map showed the interaction of *Sh*ARPC3 with other tomato proteins according to STRING database analysis. Here, the ARPC1A node in the figure represents the unknown three-dimensional (3D) structure, whereas other nodes indicate the availability of known or predicted 3D structures. The red coloured node represents the query protein. The edge, coloured in turquoise, yellow, purple, and white, indicates that the prediction was made on the basis of curated databases, text-mining, experimentally determined, and/or protein homology, respectively

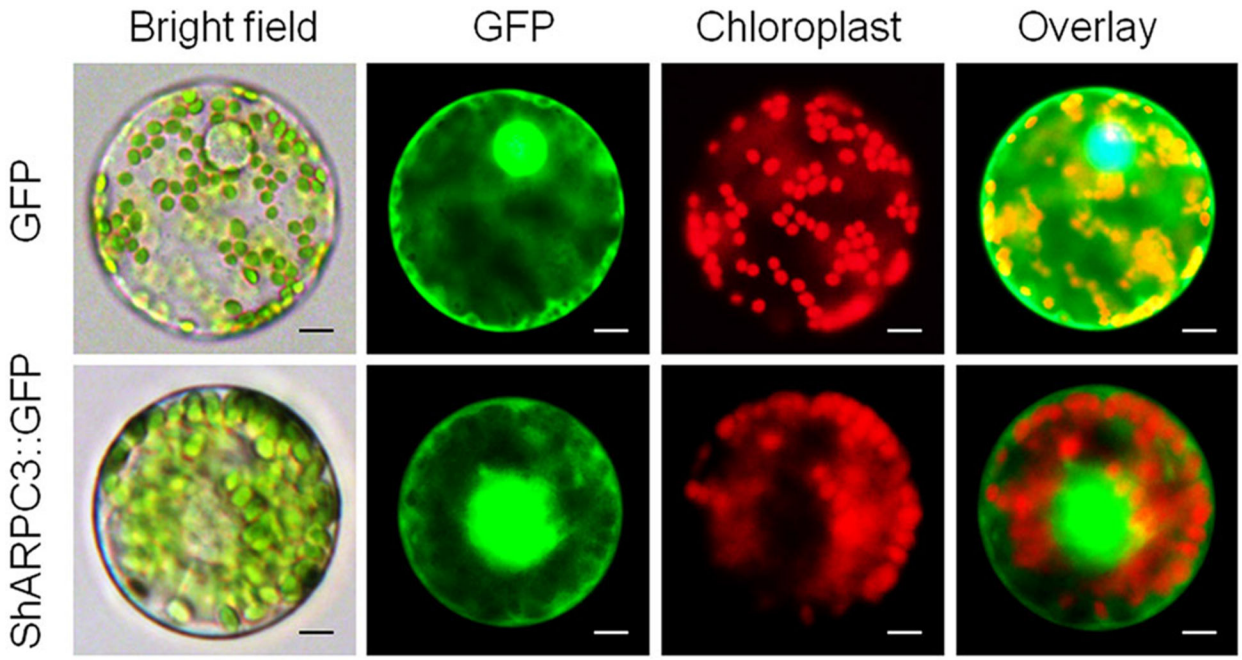

FIGURE 2.

Subcellular localization of *Sh*ARPC3. Protoplast transient expression using *GFP-ShARPC3* fusion constructs was used to determine the subcellular localization. The 35S:*GFP-ShARPC3* constructs were transformed into a tomato protoplast cell. Fluorescence images of GFP and chlorophyll autofluorescence (Chl) were captured by laser confocal scanning microscopy, as indicated by green and red emission signals, respectively (scale bars, 20 μm)

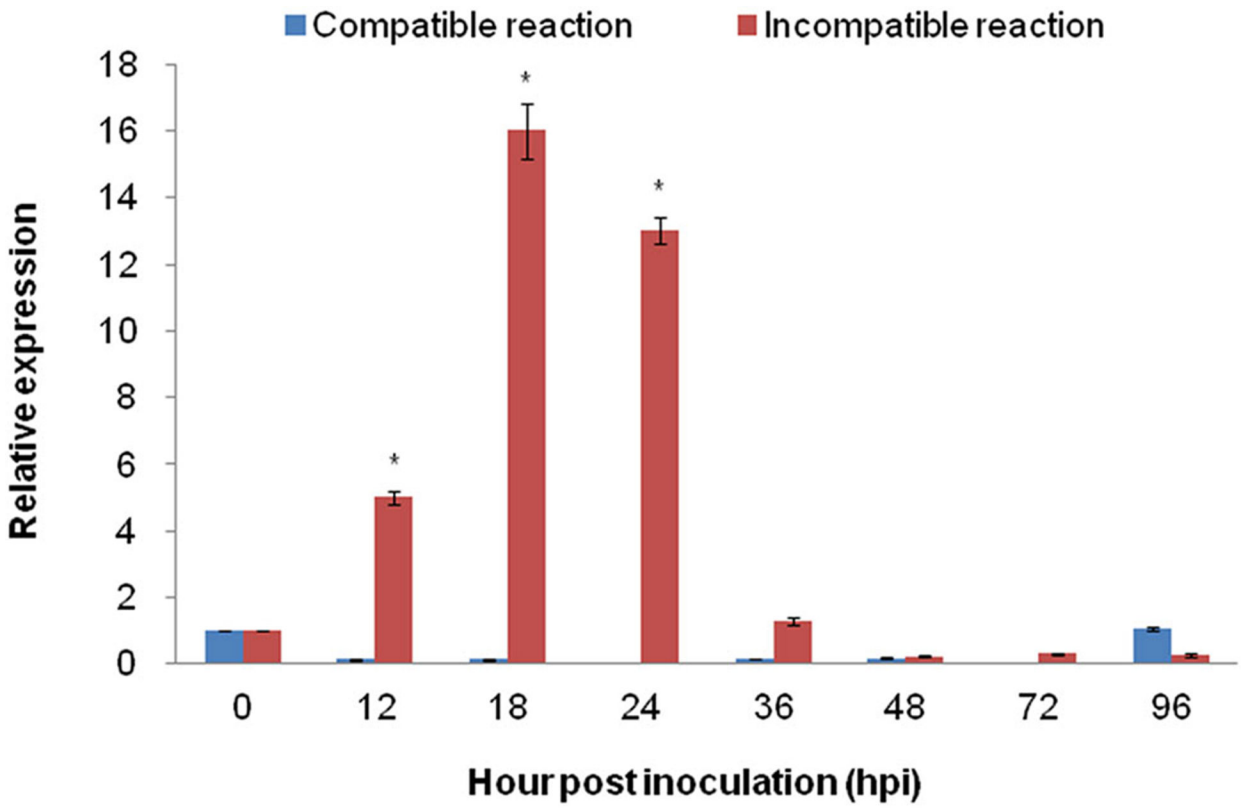

FIGURE 3.

Quantitative real-time PCR expression analysis of *ARPC3* in tomato leaves. The expression level of *ARPC3* in tomato leaves was induced in incompatible reaction between tomato-*On*-Lz interaction. Error bars represent standard deviation from three independent replicates. Asterisks (*) indicate significant difference ($P < .05$) from 0 hpi using Student's *t* test

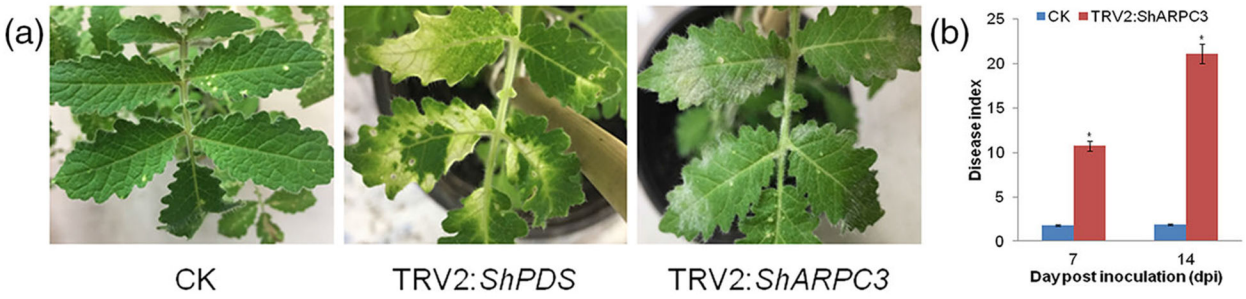

FIGURE 4.

Silencing of *ShARPC3* in tomato LA1777 renders plants susceptible to *On*-Lz. (a) Infection phenotypes of CK (TRV2), TRV2:*ShPDS*, and TRV2:*ShARPC3* tomato leaves at 7 dpi. (b) Disease indexes of CK and TRV2:*ShARPC3* plants at 7 and 14 dpi, respectively. Error bars represent the variations among three independent replicates. The asterisk (*) indicates statistically significant differences in disease index between CK (TRV2) and TRV2:*ShARPC3* plants according to independent samples *t* test ($P < .05$)

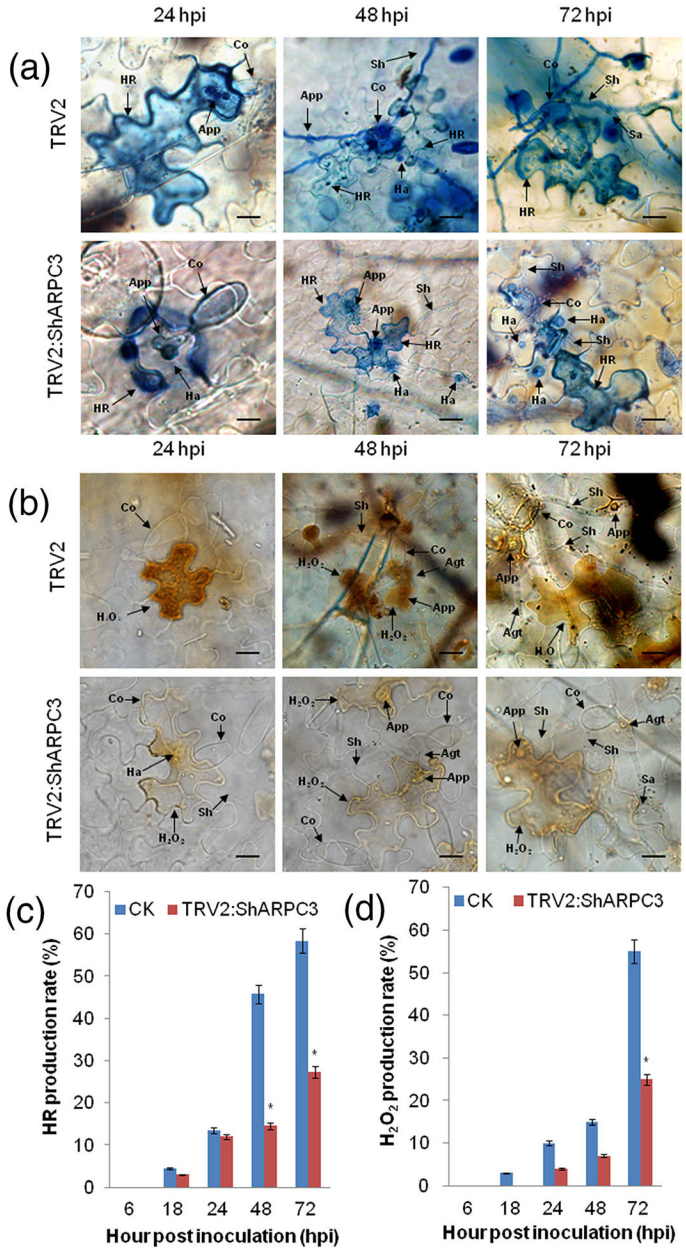

FIGURE 5.

Silencing of *ShARPC3* in tomato reduced defence responses and increased *On*-Lz infection. (a) Histological observation of hypersensitive cell death in CK (TRV2) and TRV2:*ShARPC3* tomato leaves inoculated with *On*-Lz by microscopy. Blue (trypan) staining indicates hypersensitive cell death. (b) Histological observation of H_2O_2 accumulation in CK and TRV2:*ShARPC3* tomato leaves inoculated with *On*-Lz by microscopy. (c) HR production rate of tomato leaves carrying TRV2 (CK) or TRV2:*ShARPC3* at 6, 18, 24, 48, and 72 hpi, respectively. (d) H_2O_2 production in CK or TRV2:*ShARPC3* tomato leaves at 6, 18, 24, 48, and 72 hpi, respectively. Agt, appressorium germ tube; App, appressorium; Co, conidium; Ha, haustorium; HR, hypersensitive response; Pa, papilla; Sa, secondary appressorium; Sh, secondary hyphae. Bar, 50 μm. Error bars represent the variations among three independent

replicates. The asterisk (*) indicates statistically significant differences between CK (TRV2) and TRV2:*ShARPC3* plants ($P < .05$)

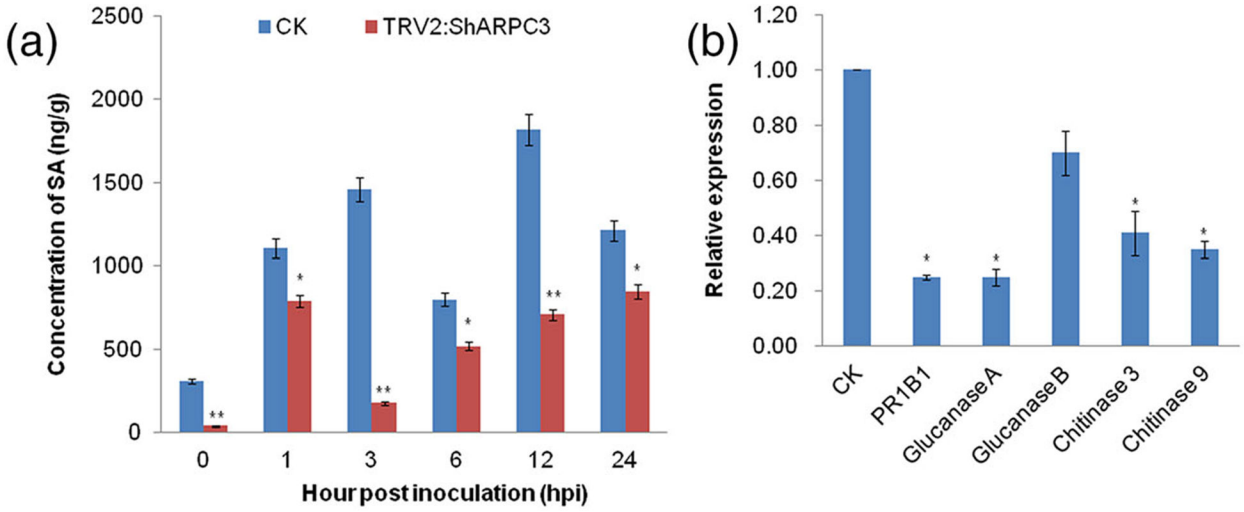

FIGURE 6.

SA content and relative mRNA transcript levels of *PRs* genes are reduced in *On*-Lz-inoculated *ShARPC3*-silenced plants. (a) Changes in SA levels in tomato leaves carrying TRV2 (CK) or TRV2:*ShARPC3* at 0, 1, 3, 6, 12, and 24 hpi, respectively. (b) Relative mRNA transcript levels of *PR1B1* (*PR1*), *β−1,3-glucanase* (*PR2*), and *chitinase* (*PR3*; SA pathway-specific gene expression markers) in CK and TRV2:*ShARPC3* tomato leaves at 24 hpi as determined by quantitative real-time PCR. Error bars represent the variations among three independent replicates. Number of asterisks indicate statistically degree of significance between CK (TRV2) and TRV2: *ShARPC3* plants (Student's *t* test, $*P < .05$; $**P < .01$)

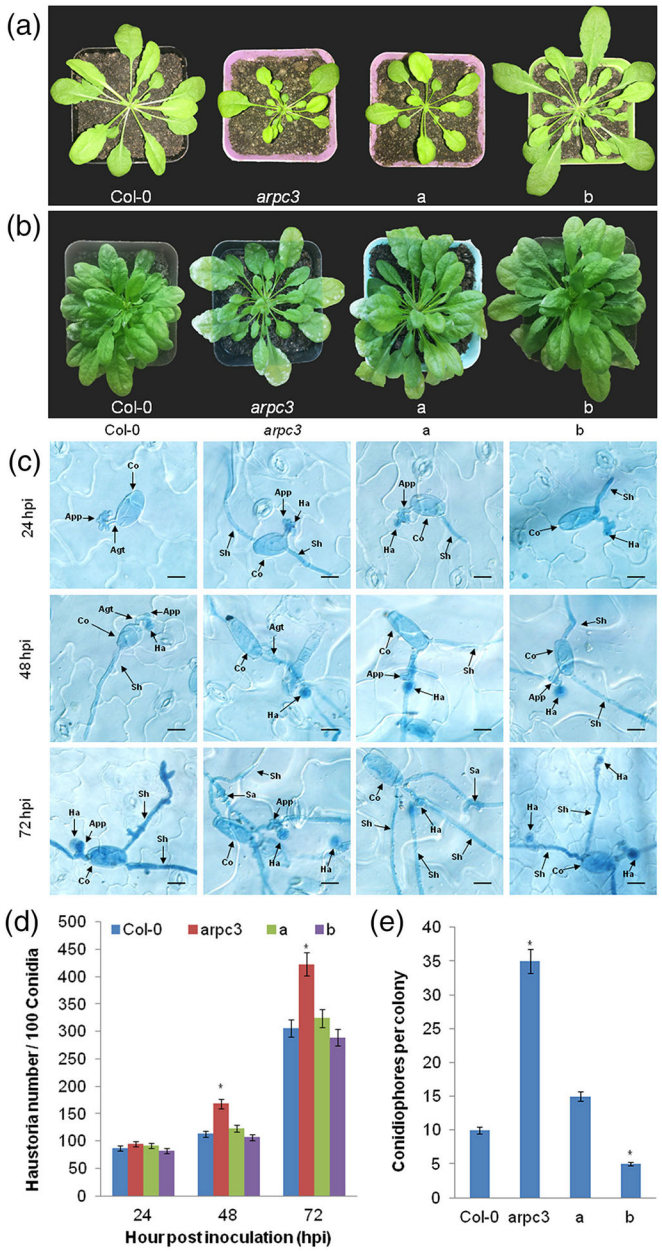

FIGURE 7.

Complementation of *ShARPC3* function confers *On*-Lz resistance in *A. thaliana*. (a) Macroscopic phenotypes of representative unchallenged plants at 8 weeks. (b) Infection phenotypes of WT Col-0 plants, *arpc3* mutants, *arpc3* plants transgenic plants expressing pCAMBIA3301-*ShARPC3*, and WT Col-0 transgenic plants expressing pCAMBIA3301-*ShARPC3*. Images were taken at 7 dpi. (c) Infection process of conidiation in WT Col-0 plants, *arpc3* mutants, *arpc3* plants transgenic plants expressing pCAMBIA3301-*ShARPC3*, and WT Col-0 transgenic plants expressing pCAMBIA3301-*ShARPC3* by microscopy. Images were taken at 24, 48, and 72 hpi. (d) Quantitative assessment of haustoria/100 conidia on WT Col-0 plants, the *arpc3* mutant, the *arpc3* mutant expressing pCAMBIA3301-*ShARPC3*, and WT Col-0 plants expressing pCAMBIA3301-*ShARPC3*.

Images were taken at 24, 48, and 72 hpi. (e) Quantitative assessment of conidiation on WT Col-0 plants, the *arpc3* mutant, the *arpc3* mutant expressing pCAMBIA3301-*ShARPC3*, and WT Col-0 plants expressing pCAMBIA3301-*ShARPC3*. Images were taken at 7 dpi. a: *arpc3* plants transgenic expressing pCAMBIA3301-*ShARPC3*; b: WT Col-0 plants expressing pCAMBIA3301-*ShARPC3*. Error bars represent the variations among three independent replicates. Asterisks (*) indicate a significant difference between WT Col-0 plants, *arpc3* mutants, *arpc3* plants expressing pCAMBIA3301-*ShARPC3*, and WT Col-0 plants expressing pCAMBIA3301-*ShARPC3* ($P < .05$)

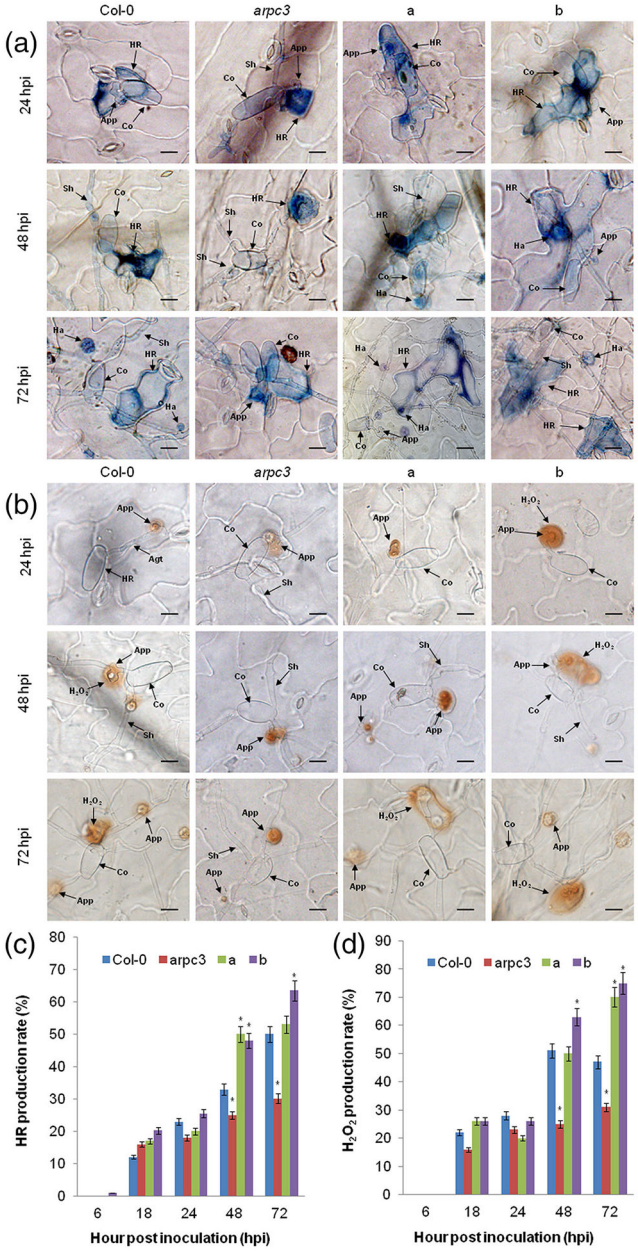

FIGURE 8.

Overexpression of *ShARPC3* in *Arabidopsis thaliana* leads to enhanced defence responses. (a) Histological observation of hypersensitive cell death in WT Col-0 plants, the *arpc3* mutant, the *arpc3* mutant expressing pCAMBIA3301-*ShARPC3*, and WT Col-0 plants expressing pCAMBIA3301-*ShARPC3* inoculated with *On*-Lz by microscopy. Blue (trypan) staining indicates hypersensitive cell death. (b) Histological observation of H_2O_2 accumulation in WT Col-0 plants, the *arpc3* mutant, the *arpc3* mutant expressing pCAMBIA3301-*ShARPC3*, and WT Col-0 plants expressing pCAMBIA3301-*ShARPC3* inoculated with *On*-Lz by microscopy. (c) HR production rate in WT Col-0 plants, *arpc3* mutants, *arpc3* transgenic plants expressing pCAMBIA3301-*ShARPC3*, and WT Col-0 plants expressing pCAMBIA3301-*ShARPC3* at 6, 18, 24, 48, and 72 hpi, respectively. (d)

H_2O_2 production rate of Col-0 plants, *arpc3* mutants, *arpc3* plants transgenic for pCAMBIA3301-*ShARPC3*, and WT Col-0 plants transgenic for pCAMBIA3301-*ShARPC3* at 6, 18, 24, 48, and 72 hpi, respectively. Agt, appressorium germ tube; App, appressorium; Co, conidium; Ha, haustorium; HR, hypersensitive response; Pa, papilla; Sa, secondary appressorium; Sh, secondary hyphae. Bar, 50 μm. a: *arpc3* plants transgenic for pCAMBIA3301-*ShARPC3*; b: WT Col-0 plants expressing pCAMBIA3301-*ShARPC3*. Error bars represent the absolute variations in conidia number among three independent biological replicates. Asterisks (*) indicate a significant difference between WT Col-0 plants and *arpc3* mutants and *arpc3* plants transgenic expressing pCAMBIA3301-*ShARPC3*, as well as WT Col-0 plants expressing pCAMBIA3301-*ShARPC3* ($P < .05$)